CrossMark

Investigation of the leaching behavior of components of the magnesium potassium phosphate matrix after high salt radioactive waste immobilization

S. E. Vinokurov[1] · S. A. Kulikova[1] · V. V. Krupskaya[2] · S. S. Danilov[1] · I. N. Gromyak[1] · B. F. Myasoedov[1]

Abstract

The samples of the magnesium potassium phosphate (MPP) matrix have been synthesized during solidification of the simulator of acid intermediate level waste. The main phase of the obtained samples corresponds to $MgK_{1-x}(NH_4)_xPO_4 \times 6H_2O$. The behavior of the matrix components during leaching with bidistilled water according to the semi-dynamic test GOST R 52126-2003 has been studied. The high hydrolytic stability of the MPP matrix to leaching of ^{137}Cs, ^{90}Sr, ^{239}Pu and ^{241}Am exceeding the stability of the cement matrix has been shown. It has been found that the components leaching process is controlled by various mechanisms due to the formation of the salts with different solubility.

Keywords Magnesium potassium phosphate matrix · Radioactive waste · Leaching rate · Leaching mechanism

Introduction

Intensive development of nuclear industry is impossible without solving the problem connecting with liquid radioactive waste (LRW) management. LRW are formed because of the activities of nuclear industry and represent a significance environmental hazard. Now, before long-term controlled storage (or disposal), LRW is recommended to be converted to solid forms, which provide maximum radioecological safety for the environment. The concept realization of safe management of LRW in Russia, which provides the complete cessation of LRW discharges into water bodies, has led to increase of the radioactive wastes nomenclature. The immediate management with some of LRW by cementing and vitrification methods is impossible due to non-compliance with regulatory requirements [1]. Primarily an intermediate level liquid (ILW) wastes with a high content of alpha-emitting nuclides (specific activity $> 10^7$ Bq l^{-1}) and ammonium nitrate can't be included in the cement matrix and can't be immobilized in aluminophosphate glass matrix because corrosion-active components (as iron and sulfates) negatively affecting the quality of glass. To solidify such ILW, it is promising to use the mineral-like magnesium potassium phosphate (MPP) matrix of the composition $MgKPO_4 \times 6H_2O$, which is synthetic analogue of the natural mineral K-struvite [2].

The MPP matrix is obtained at room temperature according to the acid–base reaction (1).

$$MgO + KH_2PO_4 + 5H_2O \rightarrow MgKPO_4 \times 6H_2O. \quad (1)$$
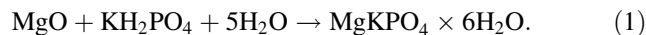
The effectiveness of the practical use of the MPP matrix was demonstrated by us earlier after solidification both imitators and real LRW [3]. It was found that the MPP matrix has significant advantages in comparison with Portland cement, including a larger solution/binder ratio (usually up to 0.8 l kg^{-1}) with high LRW salt filling (up to 30 wt%) and stability over a wide pH range of the solidified solutions.

In this article, the study results of the leaching behavior of the structure-forming elements of the MPP matrix and the radionuclides and other components of immobilized radioactive waste are presented.

✉ S. E. Vinokurov
vinokurov.geokhi@gmail.com

1   Vernadsky Institute of Geochemistry and Analytical Chemistry of the Russian Academy of Sciences, 19 Kosygin St., 119991 Moscow, Russia

2   Institute of Geology of Ore Deposits, Petrography, Mineralogy and Geochemistry of the Russian Academy of Sciences, 35 Staromonetny Per., 119017 Moscow, Russia

Experimental

Chemicals and procedures

The experiments were performed in the glove box. The strongly acid solution–simulator of evaporated raffinate of extractive refining of plutonium and neptunium *(hereinafter–Solution #1)* with a density of 1.37 ± 0.05 g cm^{-3} was used in the studies. Chemical composition of the Solution #1, g l^{-1}: HNO$_3$–300.0; H$_2$SO$_4$–150.0; NH$_4$NO$_3$–265.0; Fe(NO$_3$)$_3$–64.8; CsNO$_3$–12.8; Sr(NO$_3$)$_2$–9.6.

The preconditioning of Solution #1 for solidification was carried out by decrease of acidity to pH 2.0 ± 0.1 (to prevent ammonia emissions and iron hydrolysis) by feeding a solution of sodium hydroxide (15 mol l^{-1}) under the layer with stirring with a magnetic stirrer. To solidify the preconditioned Solution #1 according to the reaction (1) KH$_2$PO$_4$ (particle size 0.15–0.25 mm) and MgO precalcined at 1300 °C for 3 h were used. The MPP matrix samples were prepared according to reaction (1) at a solution/binder ratio of 0.68 l kg^{-1}. MgO was added in excess of 10 wt% with respect to the stoichiometry of the reaction (1), and boric acid was added in order to slow the reaction rate (1) in an amount about 1.3% of the matrix mass. The filling of the obtained samples by the Solution #1 salts was 20.8 wt%.

To study the deportment of ammonium ions after the ILW immobilization, the MPP matrix was synthesized also in a similar manner at solidification of the aqueous solution containing ammonium nitrate with a concentration of 530 g l^{-1} *(hereinafter–Solution #2)*. The samples filling with ammonium nitrate was 15.1 wt%.

As a result, after solidification Solutions #1 and 2, cubic samples of MPP matrix with dimensions of $2 \times 2 \times 2$ cm were prepared. The samples were kept for 15 days to obtain strength before studying.

To study the hydrolytic stability of the MPP matrix towards the leaching of ILW radionuclides, samples were prepared under solidification of the preconditioned Solution #1 in the same way, ^{137}Cs and ^{90}Sr were added separately in Solution #1 before solidification as well as a mixture of ^{239}Pu and ^{241}Am. Specific activity of radionuclides in Solution #1, Bq l^{-1}: ^{137}Cs–7.0×10^7; ^{90}Sr–9.8×10^7; ^{239}Pu–4.1×10^8; ^{241}Am–5.7×10^7. With the purpose of preliminary binding ^{137}Cs according to [3], nickel nitrate and potassium ferrocyanide were added to the preconditioned Solution #1, the mass of these reagents was calculated for the synthesis of cesium-potassium-nickel ferrocyanide in an amount of 1% of the matrix mass.

Methods

MPP matrix formation was controlled by X-ray diffraction (Ultima-IV, Rigaku); the Jade 6.5 (MDI) software package with a PDF-2 powder database was used to decode the obtained data. The samples structure was studied by scanning electron microscopy (SEM) (LEOSupra 50 VP, Carl Zeiss) with X-ray spectral microanalysis (X-MAX 80, Oxford Inst.).

The hydrolytic stability of the prepared samples was determined according to the semi-dynamic test GOST R 52126-2003 [4]. Test conditions: monolithic sample, leaching agent–bidistilled water (pH 6.2 ± 0.1), temperature is 23 ± 2 °C, periodic replacement of the leaching agent at 1, 3, 7, 10, 14, 21 and 28 days from the beginning of the experiment.

The matrix-forming elements content in solutions after leaching was determined by atomic-emission spectrometry with inductively coupled plasma (iCAP-6500 Duo, Thermo Scientific). The radionuclide content was determined by radiometric methods: ^{137}Cs–gamma-spectrometry (multichannel gamma spectrometer Canberra, high-purity germanium detector); ^{90}Sr–liquid-scintillation spectrometry (SKS-07P-B11(10), GreenStar, scintillator Optiphase Hi Safe III); ^{239}Pu and ^{241}Am–alpha-spectrometry (Alpha Analyst, Canberra).

Differential (LR$_{dif}$) and integral (LR$_{int}$) leaching rates of the matrix components were calculated according to Eqs. (2) and (3), respectively:

$$LR_{dif} = \frac{m_n^i}{M_0^i \cdot S \cdot \Delta t_n}, \tag{2}$$

$$LR_{int} = \frac{\sum m_n^i}{M_0^i \cdot S \cdot \Delta t_k}, \tag{3}$$

where m_n^i—the mass, g, or activity, Bq of an individual nuclide (or mixture thereof) leached for a given time interval; M_0^i—mass concentration, g g^{-1}, or specific activity Bq g^{-1} of nuclide (or mixtures thereof) in the initial sample; S—the area of the open geometric surface of the sample, contacting with water, cm^2; Δt_n—duration of the n-th leaching period between shifts of contact solution, day; Δt_k—duration of the k-th leach period from the beginning experience, day.

The leaching mechanism of matrix components was evaluated according to the model [5], which can be represented as Eq. (4):

$$\log(B_i) = A \log(t) + const, \tag{4}$$

where B_i—the total release of an element i from the sample during contact with water, mg m^{-2} or Bq m^{-2}; t—contact time, days.

Fig. 1 X-ray diffraction patterns of MPP matrix (**a**), samples obtained by solidification of Solution #1 and 2 (**b** and **c**, respectively), and comparison data of characteristic peaks (**d**)
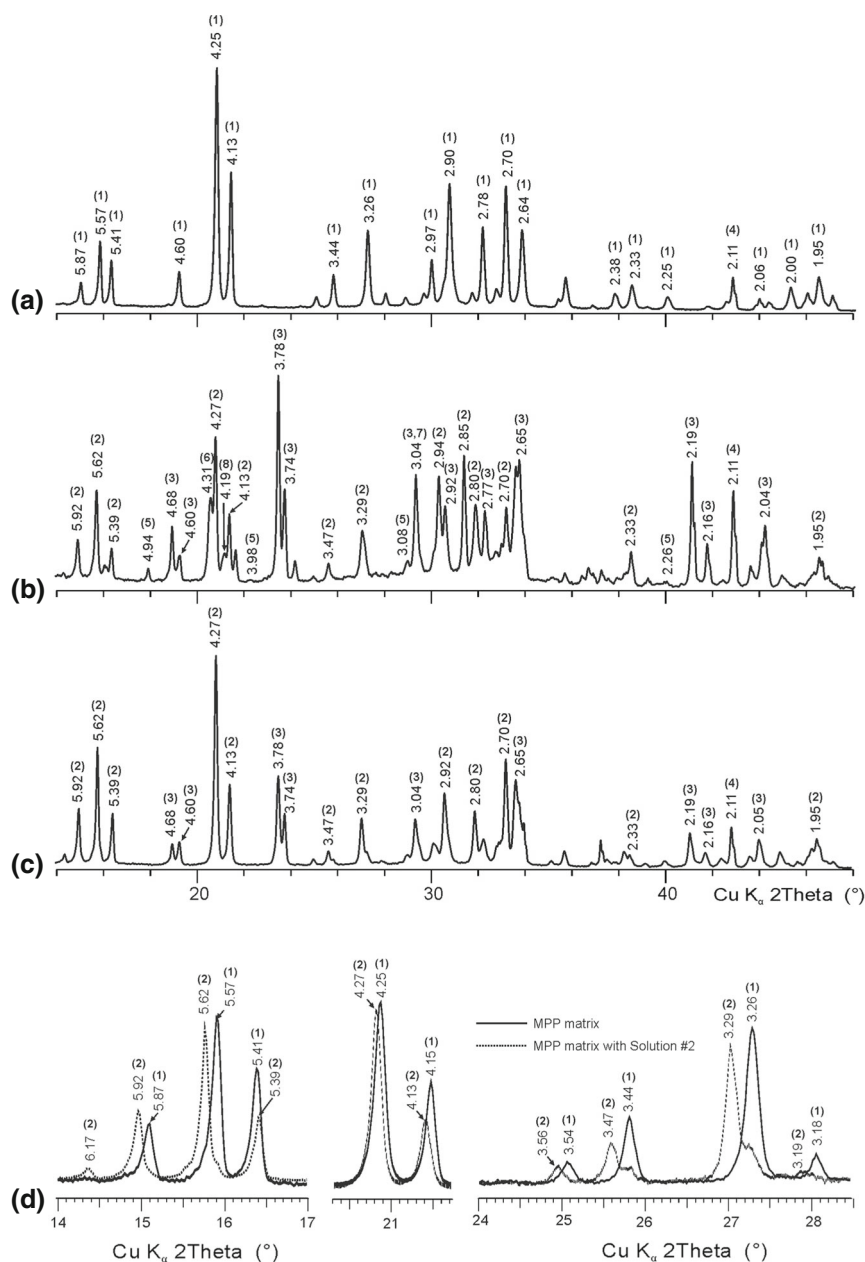
1 - $MgKPO_4 \times 6H_2O$ (K-struvite); 2 – $MgNH_4PO_4 \times 6H_2O$ (struvite); 3 – KNO_3 (niter); 4 – MgO (periclase); 5 - NH_4NO_3 (nitrammite); 6 - $MgNaPO_4$; 7 - $NaNO_3$ (nitratine); 8 – Na_3PO_4 (olympite)

The calculation of B_i was carried out according to Eq. (5):

$$B_{in} = \frac{C_{in} (L/S) (t_n)^{1/2}}{((t_n)^{1/2} - (t_{n-1})^{1/2})}, \qquad (5)$$

where C_{in}—content of element i in solutions after leaching at the end of the period n, mg l^{-1} or Bq l^{-1}; L/S—ratio of the volume of the contact solution and the surface area of

the sample, 1 m^{-2}; t_n and t_{n-1}—the total contact time for the period n and before the beginning of the period n, respectively, days.

The values of the coefficient A (slope of the line) in Eq. (2) correspond to the following element leaching mechanism: < 0.35—surface wash off (or a depletion if it found in the middle or at the end of the test); 0.35 to 0.65—diffusion transport; > 0.65—surface dissolution [6].
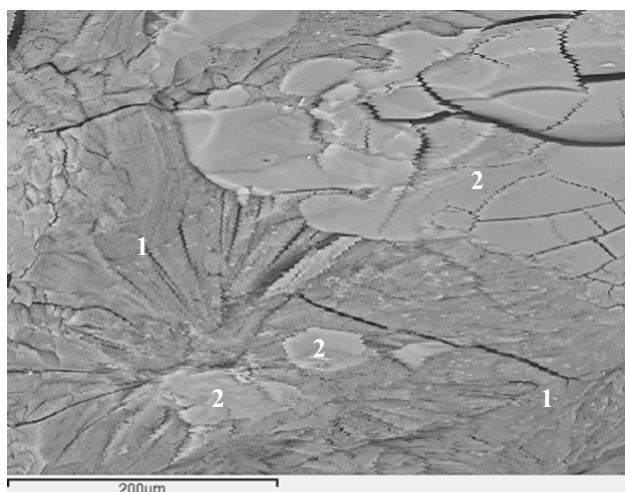
Fig. 2 SEM micrograph of the MPP matrix after Solution #2 solidification (in back-reflected electrons)

Results and discussion

The density of the obtained MPP matrix samples was 1.8 ± 0.1 g cm^{-3}. The X-ray diffraction patterns of the samples obtained by the solidification of Solutions #1 and 2 (Fig. 1b, c, respectively) in comparison with the blank MPP matrix–MgKPO$_4 \times$ 6H$_2$O (Fig. 1a) were studied. For comparison, X-ray diffraction patterns for MPP matrix and MPP matrix with Solution #2 in the ranges of 14–17, 20.5–21.5 and 24–28.5° 2θ were given. In these ranges, the most obvious difference is in the position of the characteristic phase peaks (Fig. 1d). That way, the main crystalline phase of the samples obtained during the solidification of Solutions #1 and 2 is the analogue of the natural mineral struvite, MgNH$_4$PO$_4 \times$ 6H$_2$O, which indicates the chemical bonding of ammonium ions in the
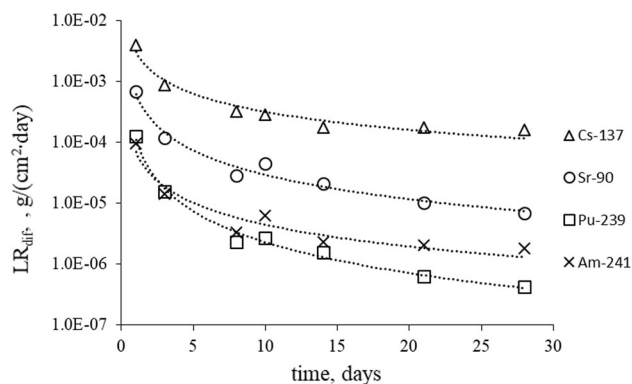

Fig. 3 Kinetic curves of the dependence of the differential leaching rate of radionuclide from the MPP matrix with immobilized Solution # 1

matrix. In addition, MgO (periclase) as well as KNO$_3$ (niter) phase were detected in these samples, the presence of which is due to the replacement of potassium by ammonium ions in the matrix MgKPO$_4 \times$ 6H$_2$O and partially by sodium in case of Solution #1 immobilization (MgNaPO$_4$ in Fig. 1b). In the samples of immobilized Solution #1 NH$_4$NO$_3$ (nitrammite), NaNO$_3$ (nitratine) and Na$_3$PO$_4$ (olympite) are also present in small quantities (Fig. 1b). Whereas other crystalline phases could not be identified, which may be due to their low content in the samples (for example, iron content in the samples 0.3 wt%) or with their weak crystallineness.

It should be noted that in the samples obtained by immobilization of Solution #2 (Fig. 1c), the individual phase of NH$_4$NO$_3$ were not found. This fact confirms the possibility of the replacement of potassium by ammonium according to reaction (6):

Table 1 Differential (LR$_{dif}$) and integral (LR$_{int}$) leaching rate of the MPP matrix components with immobilized Solution #1 according to GOST R 52126-2003 [4] on 28th day of contact with water

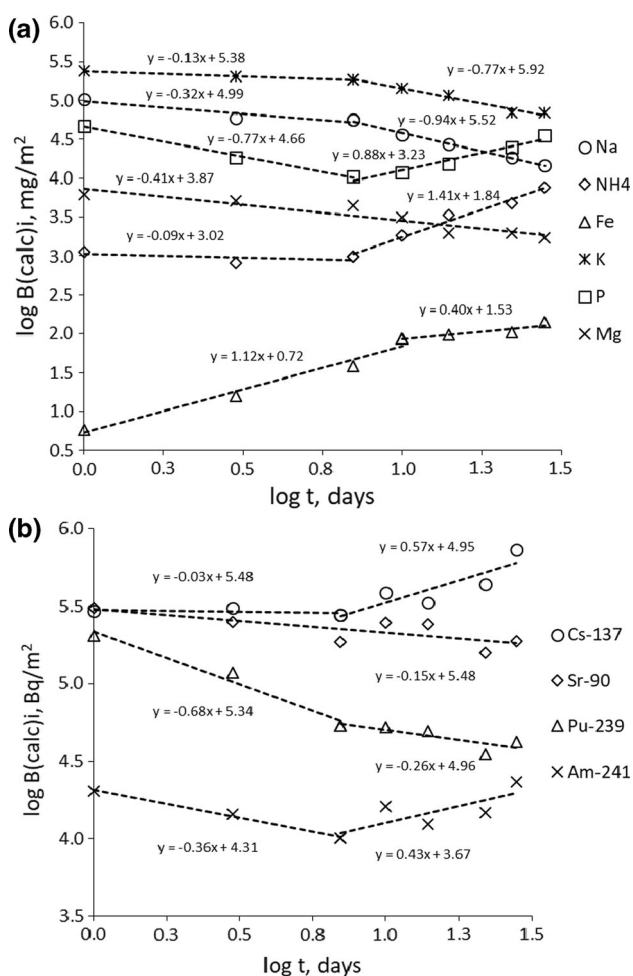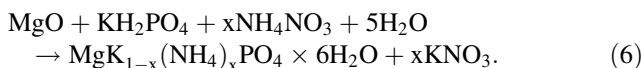| Components of the MPP matrix with immobilized Solution #1		Leaching rate, g cm^{-2} day^{-1}	
		LR$_{dif}$	LR$_{int}$
Content of matrix-forming components, wt%			
Mg	8.1	4.9×10^{-5}	5.0×10^{-4}
K	11.5	9.8×10^{-4}	1.4×10^{-2}
P	9.1	7.6×10^{-4}	2.8×10^{-3}
NH$_4$	1.2	6.9×10^{-4}	1.3×10^{-3}
Na	4.3	1.0×10^{-3}	1.4×10^{-2}
Fe	0.3	6.9×10^{-5}	8.7×10^{-5}
Specific activity of radionuclides, Bq g^{-1}			
^{137}Cs	2.6×10^{4}	1.6×10^{-4}	3.9×10^{-4}
^{90}Sr	6.9×10^{4}	6.9×10^{-6}	4.9×10^{-5}
^{239}Pu	1.6×10^{5}	4.3×10^{-7}	6.7×10^{-6}
^{241}Am	2.2×10^{4}	1.8×10^{-6}	6.8×10^{-6}

Fig. 4 Logarithmic dependence of the yield of immobilized (**a**) chemical components and (**b**) radionuclides of ILW on the time of contact of the MPP matrix samples with water

$$MgO + KH_2PO_4 + xNH_4NO_3 + 5H_2O$$
$$\rightarrow MgK_{1-x}(NH_4)_xPO_4 \times 6H_2O + xKNO_3. \qquad (6)$$

The above conclusion is supported by obtained SEM and X-ray spectral microanalysis data. The MPP matrix with immobilized Solution #2 is composed of two main phases (Fig. 2). The dark gray phase #1 consist of a mixture of phosphates with the general formula $Mg(K,NH_4,Na)PO_4 \times 6H_2O$. The atomic ratio of potassium and ammonium in individual particles reaches 0.26, which corresponds to the matrix $MgK_{0.21}(NH_4)_{0.79}PO_4 \times 6H_2O$. The light gray phase #2 is definitely KNO_3 (Fig. 2).

Based on the data on the leaching of the components of the MPP matrix with the immobilized Solution #1 (Table 1, Fig. 3), as well as the mechanism for leaching the components (Fig. 4, Table 2), the following main conclusions can be drawn.

The differences in stability of the prepared MPP matrix samples to leaching of the basic matrix-forming

Table 2 The leaching mechanism of the MPP matrix components with immobilized Solution #1

Components of the MPP matrix	Contact time of the samples with water, days	Slope of the lines (Fig. 4)	Leaching mechanism
Mg	0–28	− 0.41	Wash off
K	0–7	− 0.13	Wash off
	7–28	− 0.77	Depletion
P	0–7	− 0.77	Wash off
	7–28	0.88	Dissolution
NH$_4$	0–7	− 0.09	Wash off
	7–28	1.41	Dissolution
Na	0–7	− 0.32	Wash off
	7–28	− 0.94	Depletion
Fe	0–10	1.12	Dissolution
	10–28	0.40	Diffusion
^{137}Cs	0–7	− 0.03	Wash off
	7–28	0.57	Diffusion
^{90}Sr	0–28	− 0.15	Wash off
^{239}Pu	0–7	− 0.68	Wash off
	7–28	− 0.26	Depletion
^{241}Am	0–7	− 0.36	Wash off
	7–28	0.43	Diffusion

components—Mg, K and P were established. Differential and integral leaching rate (LR_{dif} and LR_{int}) of Mg are significantly lower than these values for K and P (Table 1), which indicates the formation by these elements of compounds with different solubilities. This confirms the data on the phase composition of the obtained samples containing both slightly soluble phosphate with the general formula $Mg(K, NH_4, Na)PO_4 \times 6H_2O$, and readily soluble salts of KNO_3, $NaNO_3$ and Na_3PO_4 (Fig. 1b). In general, it is noted that the mechanism of leaching of components can change after 7–10 days of contact of the samples with water (Fig. 4). The main contribution to the yield of K and Na from the samples is due to the rapid dissolution of their readily soluble salts when the samples begin to contact with water according to [4] and subsequent surface wash off and depletion (Fig. 4a, Table 2). The leaching mechanism of P and NH_4^+ ions on the 7th day was changed from a rapid wash off to the gradual surface dissolution, probably due to dissolution of Na_3PO_4 and unreacted NH_4NO_3, the phases of which were found in the matrix sample with immobilized Solution #1 (Fig. 1b). Higher values of the leaching rate of K and Na ions with charge (1+) in comparison with NH_4^+ ions (Table 1) confirm the predominantly binding of ammonium in the composition of a sparingly soluble phosphate, which is an analog of the mineral struvite (Fig. 1b, c).

It is established that Mg and Fe are the least leachable elements from the matrix-forming components of samples

(Table 1). Leaching of Mg by the mechanism of surface wash off under contact of the samples with water (Fig. 4a) is probably related to the formation of a small amount of easily highly soluble magnesium hydrogen phosphate $Mg(H_2PO_4)_2 \times nH_2O$ and $MgNaPO_4$ (Fig. 1). Leaching of Fe occurs probably in the first 10 days of the sample contact with water due to dissolution of iron nitrate $Fe(NO_3)_3 \times nH_2O$, and with subsequent exposure due to diffusion transport from slightly soluble Fe(III) phosphate (Fig. 4a, Table 2).

Kinetic curves of the dependence of the differential leaching rate of radionuclides from MPP matrix samples with immobilized Solution #1 are shown in Fig. 3. The values of LR_{dif} of radionuclides from the samples on the 28th day of contact with water (Fig. 3, Table 2): for ^{137}Cs and ^{90}Sr–1.6×10^{-4} and 6.9×10^{-6} g cm^{-2} day^{-1}, respectively, it is well below the permissible limit for cement matrix—1×10^{-3} g cm^{-2} day^{-1} [1]; for ^{239}Pu and ^{241}Am–4.3×10^{-7} and 1.8×10^{-6} g cm^{-2} day^{-1}, respectively (for reference: the requirement for ^{239}Pu leaching rate for glass-like matrix—$\leq 1 \times 10^{-7}$ g cm^{-2} day^{-1} [1]).

At the same time, despite the similar monotonous decrease in the LR_{dif} values of radionuclides depending on time (Fig. 3), the mechanism of their leaching from the samples of the MPP matrix differs and can vary from the time of the samples contact with water, that also was mentioned for the main matrix-forming components of the samples (Fig. 4, Table 2). It is obvious that the leaching of ^{137}Cs in the first 7 days occurs due to surface wash off similarly to K, Na and NH$_4$, and then does by the diffusion mechanism from the slightly soluble cesium-potassium-nickel ferrocyanide (Fig. 4b). The behavior of ^{90}Sr, ^{239}Pu and ^{241}Am in the first 7 days is generally similar–their release into water occurs due to surface wash. To do this, as the time of contact with water increases, the mechanisms of leaching these radionuclides differ: for ^{90}Sr due to the surface wash off; for ^{239}Pu–depletion of the surface; ^{241}Am–diffusion transport, probably from chemically resistant Am(III) orthophosphate, which is an analogue of mineral monazite.

Conclusions

The results of the performed studies demonstrate the high hydrolytic stability of the MPP matrix with immobilized ILW of complex chemical composition containing actinides; at least their stability exceeds the stability of the cement matrix. In this case it should also be noted that the use of MPP matrix is an alternative to vitrification for the salt wastes management, which contain corrosive dangerous and volatile components. This method does not require the creation of expensive high-temperature melters, the liquidation of which after the end of the service life represents a special radioecological problem and is not currently being implemented.

References

1. Federal norms and regulations in the field of nuclear energy use, NP-019-15 (2015) Collection, processing, storage and conditioning of liquid radioactive waste. Safety requirements (**in Russian**)
2. Graeser S, Postl W, Bojar H-P et al (2008) Struvite-(K), KMgPO4·6H$_2$O, the potassium equivalent of struvite—new mineral. Eur J Mineral 20:629–633
3. Vinokurov SE, Kulyako YM, Slyunchev OM et al (2009) Low-temperature immobilization of actinides and other components of high-level waste in magnesium potassium phosphate matrices. J Nucl Mater 385(1):189–192
4. GOST R 52126-2003. Radioactive waste. Determination of chemical stability of cure high level waste by method of long-term leaching. Gosstandart of Russia, Moscow (2003) (**in Russian**)
5. de Groot GJ, van der Sloot HA (1992) Determination of leaching characteristics of waste materials leading to environmental product certification. In: Gilliam TM, Wiles G (eds) Stabilization and solidification of hazardous, radioactive and mixed wastes, ASTMSTP 1123, vol 2. ASTM, Philadelphia, pp 149–170
6. Torras J, Buj I, Rovira M, de Pablo J (2011) Semi-dynamic leaching tests of nickel containing wastes stabilized/solidified with magnesium potassium phosphate cements. J Hazard Mater 186:1954–1960